BIOCHEMISTRY
including biophysical chemistry & molecular biology

Article

pubs.acs.org/biochemistry

The Catalytic Serine of *meta*-Cleavage Product Hydrolases Is Activated Differently for C−O Bond Cleavage Than for C−C Bond Cleavage

Antonio C. Ruzzini, Geoff P. Horsman,[†] and Lindsay D. Eltis*

Department of Biochemistry and Molecular Biology and Department of Microbiology and Immunology, University of British Columbia, 2350 Health Sciences Mall, Vancouver, British Columbia V6T 1Z3, Canada

Supporting Information

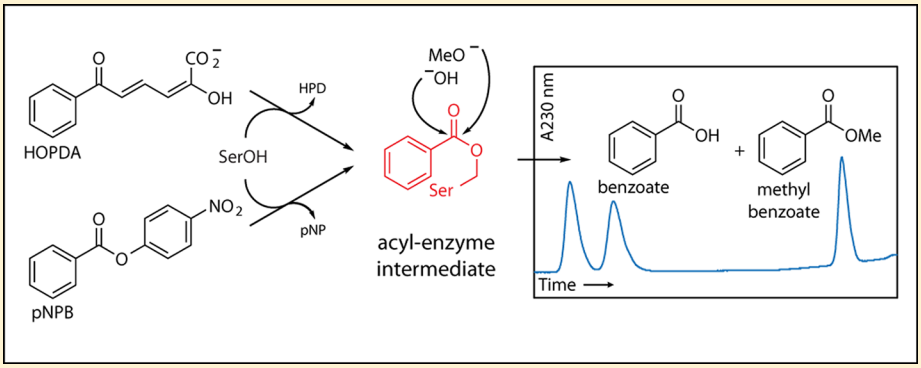

ABSTRACT: *meta*-Cleavage product (MCP) hydrolases catalyze C−C bond fission in the aerobic catabolism of aromatic compounds by bacteria. These enzymes utilize a Ser-His-Asp triad to catalyze hydrolysis via an acyl−enzyme intermediate. BphD, which catalyzes the hydrolysis of 2-hydroxy-6-oxo-6-phenylhexa-2,4-dienoic acid (HOPDA) in biphenyl degradation, catalyzed the hydrolysis of an ester analogue, *p*-nitrophenyl benzoate (pNPB), with a k_{cat} value (6.3 ± 0.5 s^{-1}) similar to that of HOPDA (6.5 ± 0.5 s^{-1}). Consistent with the breakdown of a shared intermediate, product analyses revealed that BphD catalyzed the methanolysis of both HOPDA and pNPB, partitioning the products to benzoic acid and methyl benzoate in similar ratios. Turnover of HOPDA was accelerated up to 4-fold in the presence of short, primary alcohols (methanol > ethanol > *n*-propanol), suggesting that deacylation is rate-limiting during catalysis. In the steady-state hydrolysis of HOPDA, k_{cat}/K_m values were independent of methanol concentration, while both k_{cat} and K_m values increased with methanol concentration. This result was consistent with a simple model of nucleophilic catalysis. Although the enzyme could not be saturated with pNPB at methanol concentrations of >250 mM, k_{obs} values from the steady-state turnover of pNPB at low methanol concentrations were also consistent with a nucleophilic mechanism of catalysis. Finally, transient-state kinetic analysis of pNPB hydrolysis by BphD variants established that substitution of the catalytic His reduced the rate of acylation by more than 3 orders of magnitude. This suggests that for pNPB hydrolysis, the serine nucleophile is activated by the His-Asp dyad. In contrast, rapid acylation of the H265Q variant during C−C bond cleavage suggests that the serinate forms via a substrate-assisted mechanism. Overall, the data indicate that ester hydrolysis proceeds via the same acyl−enzyme intermediate as that of the physiological substrate but that the serine nucleophile is activated via a different mechanism.

The *meta*-cleavage product (MCP) hydrolases are involved in the aerobic degradation of aromatic compounds by bacteria, cleaving a C−C bond of metabolites resulting from the dioxygenase-mediated *meta*-ring cleavage of catechols. MCP hydrolases are implicated in processes as divergent as the global carbon cycle and human health. For example, BphD is a determinant in the mineralization of polychlorinated biphenyls (PCBs),[1] while HsaD is a determinant in the catabolism of cholesterol by *Mycobacterium tuberculosis* and related pathogens.[2] In addition to their practical significance, MCP hydrolases have proven to be surprisingly interesting with respect to their catalytic mechanism and have recently provided novel insights into the versatility of the Ser-His-Asp catalytic triad.[3]

The MCP hydrolases belong to the α/β-hydrolase superfamily, which is defined by one of nature's most widespread protein folds. The α/β-hydrolase core brings a nucleophile, histidine, and an acid group together, forming a catalytic triad. Despite the members of the family sharing a common core, family specific insertions and active site loop orientation contribute greatly to the chemical diversity of this superfamily,

Received: May 21, 2012
Revised: June 27, 2012
Published: June 29, 2012

   dx.doi.org/10.1021/bi300663r | *Biochemistry* 2012, 51, 5831−5840

Scheme 1. Proposed Mechanisms of MCP Hydrolase-Mediated C−C Bond Cleavage

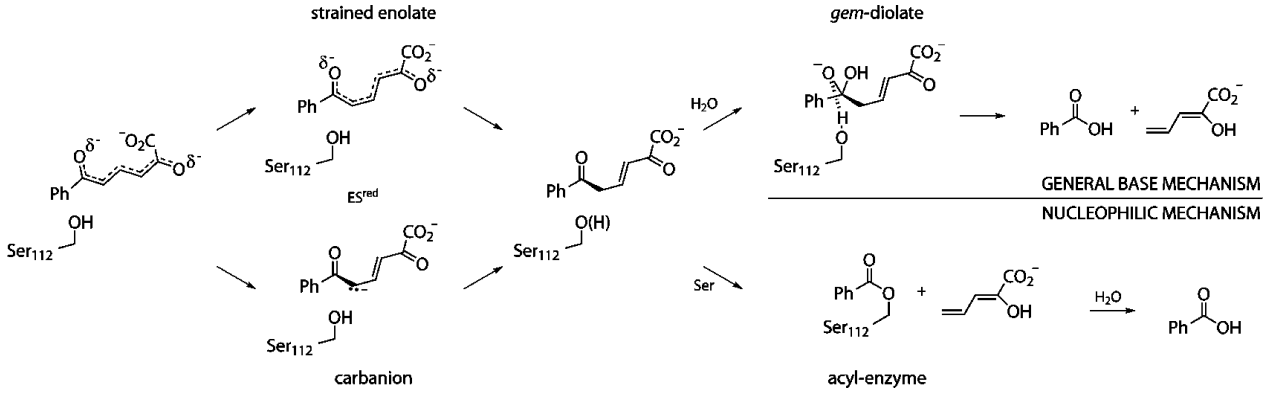

which includes haloperoxidases, dehalogenases, cofactor-less dioxygenases, and hydrolases of C−N, C−O, and C−C bonds.[4−7] Likewise, the respective catalytic mechanisms of the various families show surprising diversity despite the conserved hydrolytic machinery. Thus, while a nucleophilic mechanism has been experimentally supported for the majority of the α/β-hydrolases, at least three families utilize a general base mechanism of catalysis: hydroxynitrile lyases,[8] cofactor-less dioxygenases,[9] and enzymes such as enterobactin hydrolase that contain a His-Asp dyad but no nucleophilic residue.[10]

For more than a decade, it had been argued that MCP hydrolases utilize a general base mechanism, with hydrolysis proceeding via a *gem*-diolate intermediate.[11,12] However, chemical quench and mass spectrometry recently provided direct evidence of an acyl−enzyme intermediate in a wild-type enzyme, indicating that MCP hydrolases utilize a nucleophilic mechanism of catalysis (Scheme 1).[3] These data were obtained using BphD of *Burkholderia xenovorans* LB400, which hydrolyzes the 5,6-bond of 2-hydroxy-6-oxo-6-phenylhexa-2,4-dienoic acid (HOPDA) in biphenyl degradation with a Ser112-His265-Asp237 catalytic triad. The Ser112-benzoyl species was also trapped in crystals of a BphD H265Q variant incubated with HOPDA. Accordingly, a substrate-assisted mechanism of nucleophilic catalysis has been proposed in which Ser112 is acylated during turnover. More generally, binding of the MCP to the enzyme is thought to perturb the substrate's delocalized system of π-electrons, in part through bond strain, to catalyze the enol(ate)-to-keto tautomerization of the MCP's dienoate core (Scheme 1).[13,14] This process, which may also activate the serine for nucleophilic attack, generates a 2,6-dioxo isomer, providing an electron sink that can support carbanion formation during bond cleavage.[15,16] The mechanism of tautomerization is poorly understood, despite the latter's importance to the reaction. Remarkably, the active site of the MCP hydrolases contains five conserved residues (Asn111, Phe175, Arg190, Cys263, and Trp266) in addition to the triad, all of which directly contact the bound substrate, with the exception of Cys263.[14] Mutational analysis of these residues in either BphD or MhpC, a homologue from *Escherichia coli*, has shown that the high degree of conservation is important for C−C bond hydrolysis.[14,17] Indeed, evolutionary maintenance of the active site may reflect the difficulty associated with hydrolyzing a C−C bond, and the need for substrate tautomerization.

MCP hydrolases also mediate C−O bond hydrolysis in vitro.[18−21] This esterase activity is not surprising considering the conserved catalytic machinery of the α/β-hydrolases, which include esterases. Nevertheless, differences in the chemical nature of MCPs and esters ought to be reflected in the mechanism of hydrolysis. For example, the proposed substrate-assisted mechanism of serinate formation is dependent on the ability of these enzymes to localize charge to C5 of the MCP's dienoate core. The corresponding position in the ester substrates is an oxygen atom. More interestingly, not one of the mechanisms proposed for the MCP hydrolases invokes activation of the nucleophilic serine by the His-Asp dyad. Moreover, it has been proposed that C−O bond hydrolysis by the MCP hydrolases proceeds via a general base mechanism in which the active site serine acts as a hydrogen bond donor to a *gem*-diolate intermediate during bond cleavage.[19,21] This proposal was largely based on a Hammett analysis of the BphD-mediated hydrolysis of *para*-substituted *p*-nitrophenyl benzoates (pNPBs).

Herein, we used BphD to investigate the catalytic mechanism of C−C and C−O bond cleavage in MCP hydrolases. Steady-state kinetics and high-performance liquid chromatography (HPLC) analysis of reaction products were performed using the enzyme's physiological substrate, HOPDA, and an ester, pNPB, in the presence of small primary alcohols. The observed methanol-dependent kinetic behavior and product ratios were linked to simple kinetic models. Finally, rapid-scanning, visible absorbance spectrophotometry monitoring the pre-steady-state turnover of pNPB by the wild-type and variant enzymes was used to better define the mechanism of C−O bond hydrolysis. Together, the experiments provide new insight into the MCP hydrolase esterase activity. The mechanisms of C−C and C−O bond hydrolysis are discussed within the context of this remarkable family of enzymes.

MATERIALS AND METHODS

Chemicals and Enzyme Preparation. HOPDA was enzymatically generated from 2,3-dihydroxybiphenyl using 2,3-dihydroxybiphenyl dioxygenase as previously described.[1] All other chemicals were of analytical grade. All enzymes were purified as previously described[22] except that BphD was overproduced in Rosetta(DE3)pLysS cells (EMD4Biosciences) at 30 °C.

Enzyme Activity Measurements. Steady-state kinetic assays were performed in 1 mL of potassium phosphate (I = 0.1 M, pH 7.5) at 25 °C, unless otherwise stated. Initial reaction velocities were measured using a Cary 5000 spectrophotometer equipped with a thermostated cuvette holder. HOPDA hydrolysis was monitored at 434 nm ($\varepsilon_{434\ nm}$ = 25.7 mM^{-1} cm^{-1}), and *p*-nitrophenol production was monitored at 400 nm

dx.doi.org/10.1021/bi300663r | *Biochemistry* 2012, 51, 5831−5840

($\varepsilon_{400\ nm}$ = 12.8 mM^{-1} cm^{-1}). Steady-state rate equations were fit to individual data sets using the least-squares and dynamic weighting options of LEONORA.[23] Rate equations for specific kinetic models (*vide infra*) were fit using SCIENTIST (Micromath, St. Louis, MO).

Alcoholysis was measured at 25 and 100 mM methanol, ethanol, *n*-propanol, and 2-propanol using 4 nM BphD and 10 μM HOPDA. The methanol dependence of the steady-state kinetic turnover of HOPDA by BphD was investigated by varying the alcohol concentration between 0 and 5% (v/v; or from 0 to 1240 mM). Steady-state kinetic parameters for the BphD-mediated hydrolysis of pNPB were determined using up to 8 μM pNPB in the buffer described above supplemented with 0.2% acetone to solubilize the ester. Similarly, the methanol dependence on $v_0/[E]_T$ (k_{obs}) for pNPB turnover was measured at 2 and 4 μM ester, concentrations that were saturating in the absence of methanol.

HPLC Analysis of BphD Cleavage Products. Reactions were analyzed using a Waters 2695 HPLC system (Waters Corp., Milford, MA) equipped with a Hewlett-Packard ODS Hypersil C_{18} column (5 μM, 125 mm × 4 mm) operating at a flow rate of 1 mL/min and equilibrated at 10% solvent B (methanol) in solvent A (0.5% H_3PO_4 in H_2O). Reactions were quenched with H_3PO_4 (0.5%, v/v) and mixtures passed through a 0.45 μm filter before injection. Product ratios or percentages of acid product were calculated by measuring the amount of benzoate produced in each reaction relative to controls performed without alcohol. Control reactions in potassium phosphate (I = 0.1 M, pH 7.5) with or without 0.2% acetone were considered to be 100% hydrolytic, and the amount of benzoate was quantified by integrating the eluted peak volume using Empower 3 (Waters Corp.). All reactions analyzed using HPLC were performed in triplicate: the mean and standard deviation are reported.

Alcoholysis reactions were performed in 400 μL of potassium phosphate (I = 0.1 M, pH 7.5) at 25 °C containing 40 μM HOPDA and were initiated by adding BphD to a final concentration of 4 nM. The completeness of the reactions was judged spectrophotometrically before quenching. Samples were eluted using the following solvent gradients: (i) 10 to 30% B from 0 to 20 min, (ii) 30 to 60% B from 20 to 30 min, and (iii) 60 to 100% B from 30 to 40 min. Product elution times were as follows: 5.5 min for HPD, 13.7 for benzoate, 25.5 for methyl benzoate, 29.9 for ethyl benzoate, and 32.4 for propyl benzoate. The retention times of the alcoholytic products matched those of purchased standards.

Experiments that aimed to assess the methanol dependence of BphD-mediated hydrolysis of HOPDA and pNPB were conducted via elution using similar gradients: (i) 10 to 30% B from 0 to 20 min, (ii) 30 to 60% B from 20 to 30 min, and (iii) 60 to 100% B from 30 to 32 min. Because of the relatively low solubility of the ester, reaction volumes were increased to 1 mL and mixtures contained 4 μM pNPB. Moreover, 500 μL was injected to compensate for the reduced substrate and/or product concentration.

Stopped-Flow Spectrophotometry. Experiments were conducted using an SX.18MV stopped-flow reaction analyzer (Applied Photophysics Ltd., Leatherhead, U.K.) maintained at 25 °C by circulating water. Single turnovers of 2 μM pNPB were monitored at 400 nm using either 2, 4, or 8 μM wild-type BphD or the H265Q or H265A variant at 8 μM. Reactions were performed in triplicate using freshly prepared reagents for each replicate. Each replicate averaged the results of at least five shots and was analyzed using single- and double-exponential equations using Pro-Data Software (Applied Photophysics Ltd.). The fitted parameters from corresponding replicates were averaged, and the errors are reported as standard deviations. Similar reactions performed using the S112A variant (8 μM BphD and 2 μM pNPB) were monitored using a Cary 5000 spectrophotometer. Finally, reactions performed using excess ester (0.1, 0.25, or 0.5 μM BphD and 2 μM pNPB) were also analyzed at 400 nm using the stopped-flow instrument. Burst and double-exponential equations were fit to replicate data sets.

RESULTS

BphD Cleaved HOPDA and pNPB with the Same k_{cat}. To investigate C−O bond hydrolysis by the MCP hydrolases, we measured the ability of BphD to hydrolyze pNPB, an ester that shares a chemical substructure with HOPDA. The BphD-mediated hydrolysis of pNPB obeyed Michaelis−Menten kinetics, and the resulting fitted parameters were as follows: k_{cat} = 6.3 ± 0.5 s^{-1}, k_{cat}/K_m = 19 ± 3 μM^{-1} s^{-1}, and K_m = 0.34 ± 0.02 μM. Under nearly identical conditions (with or without 0.2% acetone), BphD hydrolyzed HOPDA at essentially the same rate (k_{cat} = 6.5 ± 0.5 s^{-1}).

While the essentially identical k_{cat} values for the hydrolysis of HOPDA and pNPB could have a variety of origins, we hypothesized that it was due to the rate-limiting breakdown of a shared acyl−enzyme intermediate. To test this hypothesis, we tested the ability of BphD to utilize methanol as an alternative acceptor. Products resulting from the turnover of 40 μM HOPDA or 4 μM pNPB in the presence of 25 mM methanol were analyzed by HPLC. In both reactions, equal amounts of benzoate and methyl benzoate were produced: benzoic acid accounted for 48 ± 2 and 49 ± 1% of the benzoyl-containing product from the cleavage of HOPDA and pNPB, respectively (Figure S1 of the Supporting Information).

Short-Chain, Primary Alcohols Accelerated the Turnover of HOPDA. To further characterize the observed mechanism of alcoholysis and the event associated with k_{cat}, we tested the ability of BphD to utilize other alcohols during the steady-state turnover of HOPDA. The effects of several alcohols on the initial velocity (v_0) of BphD-catalyzed turnover of 10 μM HOPDA were measured. In the absence of alcohol, v_0 was 25 ± 1 μM s^{-1} [k_{obs} ~ 6 s^{-1} (Table 1)]. Concentration-dependent increases in v_0 were apparent upon the addition of either methanol, ethanol, or *n*-propanol. The observed effects ranged from an approximate 3.2-fold increase in the presence of 100 mM methanol to a more modest 1.2-fold increase at the

Table 1. Effects of Alcohol on BphD-Mediated C−C Bond Hydrolysis[a]

	[alcohol] (mM)	v_0 (μM s^{-1})	acid:ester product ratio
methanol	0	25 ± 1	
	25	45.8 ± 0.7	1.06 ± 0.01
	100	76 ± 1	0.24 ± 0.01
ethanol	25	29.4 ± 0.9	3.78 ± 0.05
	100	45.9 ± 0.7	0.95 ± 0.02
n-propanol	25	26.0 ± 0.6	42.8 ± 0.8
	100	29 ± 1	3.57 ± 0.07
2-propanol	25	25.8 ± 0.6	ND[b]
	100	25.5 ± 0.3	ND[b]

[a]Distinct experiments were used to measure v_0 (10 μM HOPDA) and product ratios (40 μM HOPDA). [b]Not detected.

dx.doi.org/10.1021/bi300663r | *Biochemistry* 2012, 51, 5831−5840

same concentration of *n*-propanol. Inspection of the series indicates that the values of v_0 reflect the pK_a of the substituting nucleophile. Importantly, v_0 was not significantly affected by the addition of 25 or 100 mM 2-propanol, suggesting that the tested alcohols compete to replace the nucleophilic water and do not contribute any allosteric effects that accelerate the reaction.

In addition to the observed kinetic phenomena, HPLC analysis of the reaction products was used to correlate the observed accelerations in v_0 directly to alcohol utilization by BphD (Table 1). Specifically, we observed that partitioning between the hydrolytic and alcoholytic reaction pathways was linked to common v_0 measurements. For instance, using either 25 mM methanol or 100 mM ethanol, the acid:ester ratio was ~1 and $v_0 \sim 46$ μM s^{-1}. Similarly, the same v_0 was observed using 25 mM ethanol and 100 mM *n*-propanol (~29 μM s^{-1}), and the acid:ester product ratio was ~3.6.

Methanolysis Provided Indirect Evidence of a Shared Intermediate. The remarkably similar k_{cat} values for the hydrolysis of HOPDA and pNPB and the results of the alcoholysis experiments suggested that the BphD-catalyzed reactions involve the rate-determining breakdown of a shared catalytic intermediate, such as a benzoyl−enzyme intermediate. To investigate this possibility, we studied the effect of variable methanol concentrations on the steady-state kinetic parameters and product ratios for the BphD-catalyzed transformation of HOPDA (Figure 1). Significantly, k_{cat} and K_m increased with

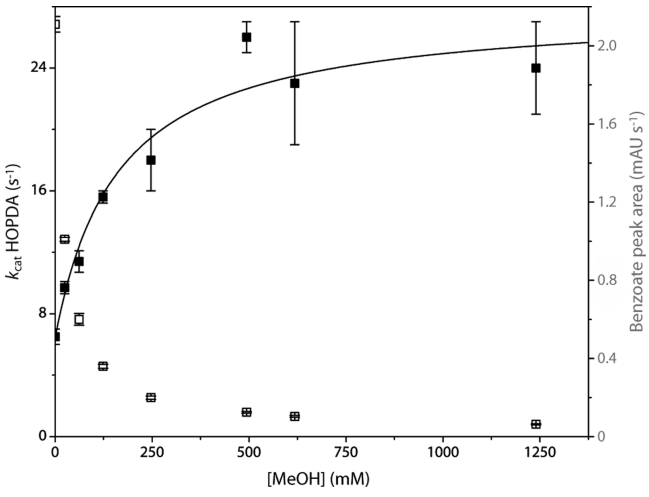

Figure 1. Dependence of k_{cat} on methanol concentration for the BphD-catalyzed transformation of HOPDA. The solid line represents the fit of the steady-state rate equation for the nucleophilic mechanism (Scheme 3, eq 4) to the experimentally determined k_{cat} values for HOPDA depletion (■). The fitted parameters were as follows: $k_2 = 30 \pm 3$ s^{-1}, $k_3[H_2O] = 8 \pm 3$ s^{-1}, and $k_4 = 230 \pm 80$ M^{-1} s^{-1}. Values from the quantification of benzoate at the varied methanol concentrations are shown in white (□). The area of each peak was calculated as a function of the voltage per second and then converted to milli-absorbance units per second.

methanol concentration while k_{cat}/K_m remained unchanged (Table 2). The experimentally determined values were compared to those predicted from kinetic models based on each of the general base and nucleophilic mechanisms. Steady-state rate expressions for partitioning in each of the two mechanisms are shown in Schemes 2[24] and 3,[25] respectively. A cursory inspection of the rate equations reveals that only the nucleophilic mechanism correctly predicts the methanol independence of the k_{cat}/K_m values, as $k_{cat}/K_m = k_2/K_S$. In contrast, the general base mechanism predicts that this parameter should increase with methanol concentration.

Further inspection reveals that the model based on a nucleophilic mechanism is better able to account for the experimental data in several other respects. In this model, k_{cat} for HOPDA depletion is described by eq 4, with the following fitted values: $k_2 = 30 \pm 3$ s^{-1}, $k_3[H_2O] = 8 \pm 3$ s^{-1}, and $k_4 = 230 \pm 80$ M^{-1} s^{-1} (Scheme 2). These rate constants allow the calculation of k_{cat} values specific for acid and ester formation, which were used to predict product ratios at each methanol concentration (Table 2). Indeed, the product ratios predicted by the model are in good agreement with the experimentally measured amounts of benzoate produced during steady-state turnover of HOPDA (Table 2 and Figure S1 of the Supporting Information). The k_{cat}/K_m value, ~25 μM^{-1} s^{-1}, also provides an estimate of K_S for the nucleophilic mechanism, allowing a comparison of predicted and experimental K_m values. Simplifying k_{cat}/K_m for HOPDA to k_2/K_S and substituting a k_2 of 30 s^{-1} yields a K_S of 1.2 μM. Subsequent predictions of the methanol-dependent K_m values from K_S are consistent with the experimental values (Table 2).

To further investigate the mechanism of C−O bond cleavage, we also measured the methanol dependence of pNPB turnover by BphD (Table 3 and Figure 2). Unfortunately, the relatively low solubility of pNPB precluded reliable determination of the steady-state kinetic parameters in the presence of methanol. Despite this limitation, the rate of BphD-catalyzed C−O bond cleavage at 2 and 4 μM pNPB provided some mechanistic insight. As we observed for the transformation of HOPDA, the rate of pNPB turnover increased with methanol concentration. However, the k_{obs} value also decreased at methanol concentrations >250 mM, reflecting an increase in the $K_{m\ pNPB}$ as observed for HOPDA turnover. At lower methanol concentrations, the k_{obs} values for pNPB turnover were within error of the k_{cat} values determined for HOPDA. Furthermore, the methanol-dependent product formation, as measured by HPLC, indicated that the partitioning ratio was equal to that observed for HOPDA (Table 3).

Activation of the Serine Nucleophile for C−O Bond Hydrolysis. While the alcohol-dependent steady-state kinetic data suggest that both the C−O and C−C hydrolytic reactions proceed through an acyl−enzyme intermediate, they do not establish the mechanism of nucleophile activation. Accordingly, we further probed the mechanism of ester bond hydrolysis using stopped-flow, visible spectrophotometry to monitor the hydrolysis of pNPB by BphD and three catalytic triad variants: H265Q, H265A, and S112A. The turnover of 2 μM pNPB by 1 or 2 equivalents of WT BphD resulted in the biphasic production of pNP (Table 4 and Figure 3) reminiscent of HPD formation during HOPDA turnover.[13] Interestingly, turnover of pNPB by a 4-fold excess of enzyme resulted in monophasic formation of pNP at a rate approximately 5-fold faster than the second phase of turnover observed at equimolar concentrations of enzyme and pNPB. Even at equal reactant concentrations, k_2 was approximately 7-fold faster than k_{cat}, suggesting that an additional process, downstream of pNP release, is rate-determining but cannot be observed at 400 nm during a single turnover. Again, these results support the rate-limiting breakdown of an acyl−enzyme intermediate during BphD-catalyzed C−O bond cleavage.

Table 2. Experimentally Observed and Calculated Steady-State Kinetic Parameters for the Methanol-Dependent BphD-Catalyzed Transformation of HOPDA[a]

	experimental				calculated[b]				
[MeOH] (mM)	k_{cat} (s^{-1})	K_m (μM)	k_{cat}/K_m (μM^{-1} s^{-1})	% acid	k_{cat} (s^{-1})	$k_{cat\ acid}$ (s^{-1})	$k_{cat\ ester}$ (s^{-1})	K_m (μM)	% acid
0	6.5 ± 0.5	0.20 ± 0.05	32	0 ± 2	6.5	6.5	0	0.26	0
25	9.4 ± 0.5	0.4 ± 0.1	27	48 ± 2	9.6	5.7	3.9	0.38	59
62	13	0.60	22	27 ± 2	13	4.7	8.2	0.52	37
124	16	0.83	19	17 ± 1	17	3.7	13	0.66	23
247	21 ± 4	0.8 ± 0.2	26	10 ± 1	21	2.6	18	0.82	13
494	26	0.85	31	5.8 ± 0.3	24	1.6	22	0.96	7
618	21 ± 5	0.99 ± 0.07	21	4.9 ± 0.3	25	1.4	24	1.0	5
1240	28 ± 4	2.0 ± 0.4	14	3.0 ± 0.2	27	0.8	26	1.1	3

[a]Standard errors are reported for kinetic parameters; values without an error represent a single measurement. Errors for product analysis are reported as standard deviations calculated from three independent samples. [b]Calculated using the equations for the nucleophilic mechanism in Scheme 2: k_2 = 30 s^{-1}, $k_3[H_2O]$ = 8.3 s^{-1}, k_4 = 230 M^{-1} s^{-1}, and K_S = 1.2 μM.

Scheme 2. Steady-State Rate Expressions for a Simple Model of Nucleophilic Catalysis

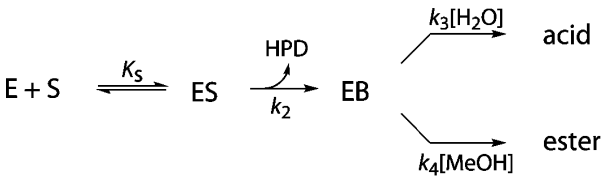

$$K_m = K_S \frac{k_3[H_2O] + k_4[MeOH]}{k_2 + k_3[H_2O] + k_4[MeOH]} \quad \text{eq 1}$$

$$k_{cat(acid)} = \frac{k_2 k_3[H_2O]}{k_2 + k_3[H_2O] + k_4[MeOH]} \quad \text{eq 2}$$

$$k_{cat(ester)} = \frac{k_2 k_4[MeOH]}{k_2 + k_3[H_2O] + k_4[MeOH]} \quad \text{eq 3}$$

$$k_{cat(HOPDA)} = \frac{k_2 k_3[H_2O] + k_2 k_4[MeOH]}{k_2 + k_3[H_2O] + k_4[MeOH]} \quad \text{eq 4}$$

Scheme 3. Steady-State Rate Expression for a Simple Model of General Base Catalysis

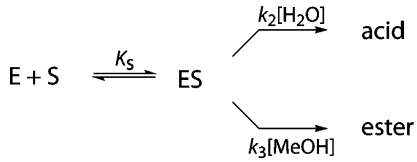

$$k_{cat}/K_m = \frac{k_2[H_2O] + k_3[MeOH]}{K_S} \quad \text{eq 5}$$

Table 3. Experimentally Observed Methanol-Dependent Rates ($k_{obs} = v_i/[E]_T$) of pNPB Transformation by BphD

	k_{obs} (s^{-1})		
[MeOH] (mM)	2 μM pNPB	4 μM pNPB	% acid at 4 μM pNPB
0	6.4 ± 0.3	6.5 ± 0.1	0 ± 1
25	9.9 ± 0.5	10.7 ± 0.5	49 ± 1
62	12.8 ± 0.2	14.6 ± 0.3	29 ± 1
124	16 ± 1	18.4 ± 0.1	20 ± 1
247	17 ± 2	21 ± 1	14.4 ± 0.7
618	14 ± 1	20.1 ± 0.8	5.7 ± 0.3
1240	11 ± 1	17.0 ± 0.4	3.7 ± 0.2

For the sake of simplicity, subsequent experiments were performed using a 4-fold excess of enzyme to substrate. Substitution of Ser112 with alanine resulted in the near abrogation of C−O bond cleavage ($k \sim 10^{-4}$ s^{-1}). Furthermore, the rates of ester bond hydrolysis were reduced by at least 3 orders of magnitude for the His265 variants. Specifically, the H265A and H265Q variants cleaved pNPB at rates of 0.06 and 0.014 s^{-1}, respectively (Table 4).

Biphasic Pre-Steady-State Formation of pNP. To investigate the biphasic product release observed during single-turnover experiments, we monitored the turnover of 4-, 8-, and 20-fold excesses of pNPB by BphD. In all cases, the kinetic traces monitoring multiple pNPB turnovers were biphasic (Figure 4) and could be modeled by either burst or double-exponential equations (Table 5 and Figure S2 of the Supporting Information). Fitting a burst equation to the data

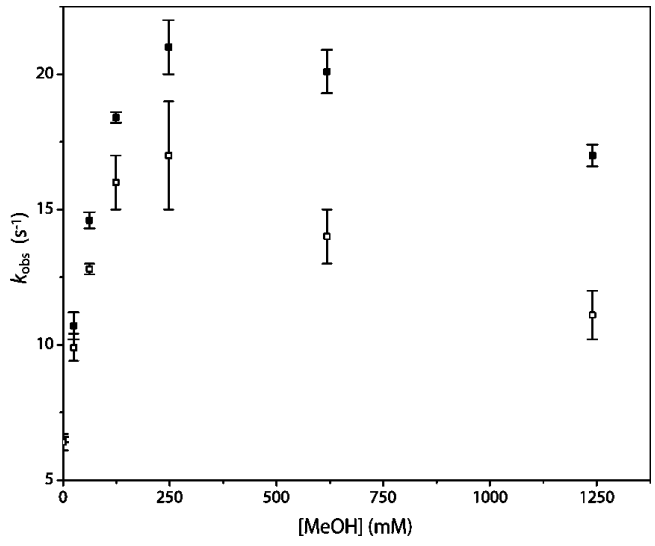

Figure 2. Methanol-dependent BphD-mediated cleavage of pNPB. The experimentally observed rates (k_{obs}) represent $v_0/[E]_T$ at 2 (□) and 4 μM pNPB (■).

dx.doi.org/10.1021/bi300663r | Biochemistry 2012, 51, 5831−5840

Table 4. Kinetic Data for pNPB Turnover by Wild-Type BphD and Its Variants

[E]:[pNPB]	k_1 (s^{-1}) (% Amp)	k_2 (s^{-1}) (% Amp)
1 WT	210 ± 40 (18)	41 ± 5 (82)
2 WT	170 ± 10 (38)	74 ± 2 (62)
4 WT	206 ± 5...	
4 H265Q	0.014 ± 0.002	
4 H265A[a]	0.06	
4 S112A[b]	0.00016 ± 0.00002	

[a]Data reported for a single replicate. [b]Value measured using a Cary 5000 spectrophotometer.

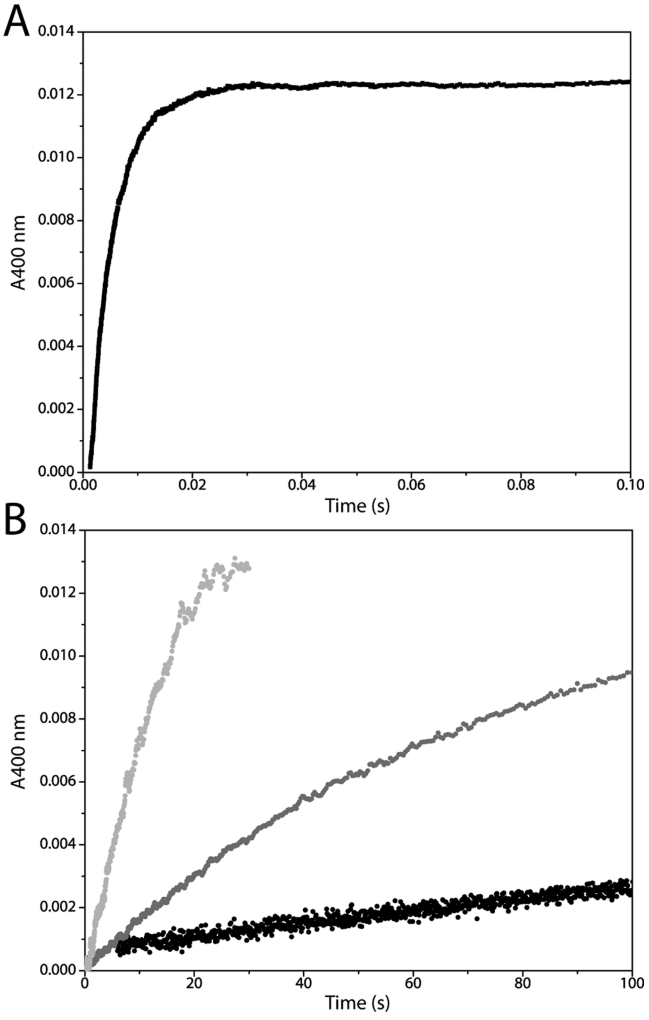

Figure 3. Representative single turnover of pNPB by a 4-fold excess of BphD. (A) For WT, $k \sim 200$ s^{-1}. (B) For H265A, $k \sim 0.06$ s^{-1} (light gray). For H265Q, $k \sim 0.014$ s^{-1} (dark gray). For S112A, $k \sim 0.0002$ s^{-1} (black).

revealed that the rates of pNP formation during the burst phase ($k_{burst} \sim 42$ s^{-1}) and the steady-state phase ($k_{ss} \sim 8$ s^{-1}) were independent of enzyme concentration. This analysis also indicated that the amount of pNP formed during the burst phase corresponded to ~70% of the enzyme present in the assay. Similarly, analysis using a double-exponential equation implied that ~60% of the enzyme was active during the pre-steady-state phase (k_1) which proceeded at a rate of ~50 s^{-1}, in relatively good agreement with k_{burst} and k_2 during a single turnover of pNPB at a 1:1 ratio with BphD. In contrast, values

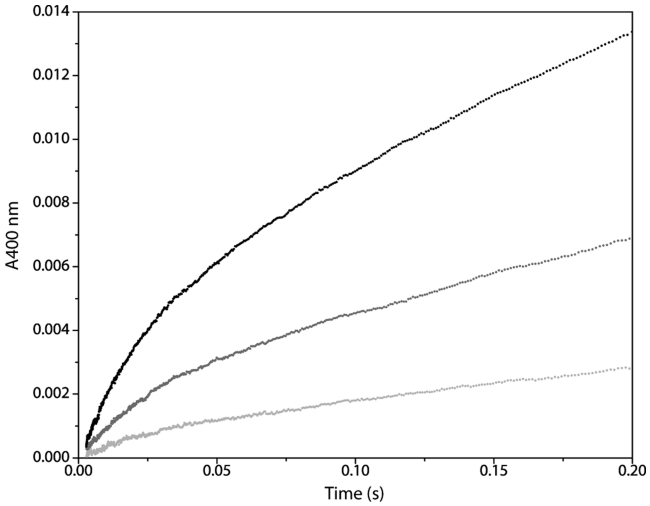

Figure 4. Representative stopped-flow experiments demonstrating the pre-steady-state formation of pNP by BphD in potassium phosphate buffer (I = 0.1 M, pH 7.5) and 0.2% (v/v) acetone at 25 °C. The hydrolysis of 2 μM pNPB was monitored using 0.1 (light gray), 0.25 (dark gray), and 0.5 μM BphD (black).

of k_2 from the fit of a double-exponential equation to the multiple-turnover data, from 0.8 to 2.8 s^{-1}, demonstrated a dependence on enzyme concentration and were significantly lower than the experimentally determined k_{cat} value of 6.5 s^{-1}. The "burst-like" kinetic behavior observed for pNPB turnover is consistent with rate-limiting deacylation. Nevertheless, the magnitude of the pre-steady-state burst of pNP formation appears to be substoichiometric, but significantly higher than the value of 50% predicted from the two-conformation model proposed for C−C bond hydrolysis.

DISCUSSION

The alcoholysis experiments presented herein provide additional evidence of covalent catalysis in the MCP hydrolases, supporting the idea that the hydrolysis of esters by these enzymes also involves an acyl−enzyme intermediate. Thus, the similar k_{cat} values for the hydrolysis of HOPDA and pNPB and the similar partitioning of their products to benzoate and methyl benzoate indicate that both C−C and C−O bond cleavage proceed through a shared intermediate. Moreover, the steady-state kinetic analysis of methanolysis and propanolysis provides indirect evidence that the shared intermediate is an acyl−enzyme intermediate. This builds on the direct observation of a Ser112−benzoyl species by chemical quench MS in WT BphD, its observation in the H265Q variant using crystallography,[3] and indirect evidence of its occurrence, including the stoichiometric incorporation of ^{18}O from $H_2{}^{18}O$ during turnover and the appearance of a pre-steady-state kinetic burst. Finally, the methanolysis and propanolysis data further indicate that k_{cat} represents the rate-limiting breakdown of the acyl−enzyme intermediate.

The observed accelerations in the initial velocities and the ability of BphD to utilize longer alcohols, such as *n*-propanol, are consistent with covalent catalysis. The crystal structure of BphD S112A in complex with HOPDA revealed a complex suite of interactions,[17,26] reflecting the high degree of active site residue conservation. Little residual volume is present within the occupied active site, suggesting that acylation and release of HPD precede the binding of additional nucleophiles such as

dx.doi.org/10.1021/bi300663r | *Biochemistry* 2012, 51, 5831−5840

Table 5. Pre-Steady-State Kinetic Parameters Derived from Monitoring *p*NB Formation at 400 nm[a]

Fits to a Burst Equation					
[E] (μM)	k_{burst} (s^{-1})	Amp_{burst} (ΔA_{400})	$[pNP]_{burst}$ (μM)	k_{ss} (ΔA_{400} s^{-1})	k_{ss} (s^{-1})
0.10	42 ± 3	0.00077 ± 0.00004	0.060 ± 0.003	0.0101 ± 0.0005	7.9 ± 0.4
0.25	41 ± 4	0.0022 ± 0.0001	0.17 ± 0.01	0.024 ± 0.001	7.4 ± 0.4
0.50	44 ± 5	0.0044 ± 0.0003	0.35 ± 0.02	0.046 ± 0.001	7.1 ± 0.2
Fits to a Double-Exponential Equation					
[E] (μM)	k_1 (s^{-1}) (% Amp)	$[pNP]_{k_1}$ (μM)	k_2 (s^{-1}) (% Amp)	$[pNP]_{total}$[b] (μM)	
0.10	44 ± 2 (5)	0.059 ± 0.004	0.8 ± 0.1 (90)	1.2 ± 0.2	
0.25	47 ± 6 (8)	0.152 ± 0.007	1.4 ± 0.1 (92)	1.8 ± 0.1	
0.50	60 ± 10 (12)	0.27 ± 0.02	2.8 ± 0.4 (88)	2.2 ± 0.3	

[a]Errors associated with amplitudes were <12%. [b]$[pNP]_{total}$ was calculated on the basis of the fitted amplitudes.

Scheme 4. Nucleophilic Mechanism for C−C and C−O Bond Cleavage

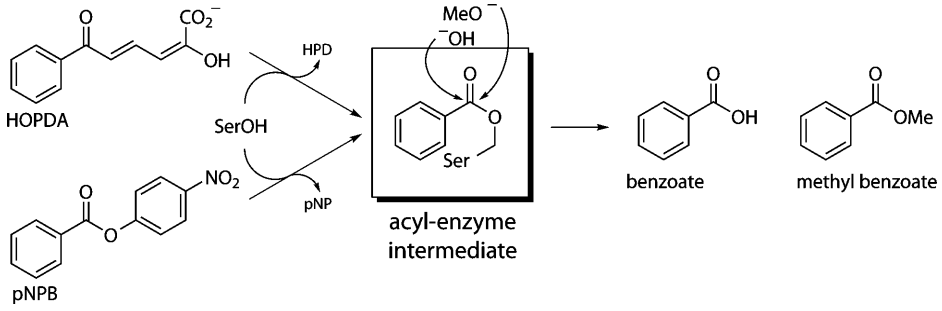

water or alcohols. Indeed, product inhibition studies support a mechanism in which HPD is released before benzoate during turnover of HOPDA.[13] In contrast, significant movement of the MCP hydrolase lid domain (residues 146−211) would be required to bind additional molecules to a HOPDA-occupied active site. Considering the full suite of interactions within the enzyme−substrate complex, it is difficult to conceive how such lid movement would not disrupt productive substrate binding.

The alcohol-dependent acceleration of v_0 provides novel insight into the MCP hydrolase catalytic cycle inasmuch as it suggests that the breakdown of the acyl−enzyme intermediate is rate-limiting. To date, experiments in MhpC and BphD have assigned k_{cat} to either release of the noncovalently bound product[16,19] or a conformational change associated with chemistry.[13] The observed increase in the rate of turnover in the presence of alternate acceptors suggests breakdown of the acyl−enzyme intermediate rather than product release limits catalysis. Indeed, the methanol-induced rate acceleration (28 s^{-1} vs 6.5 s^{-1}) is similar in magnitude to that reported for the turnover of an ester substrate by α-chymotrypsin (482 s^{-1} vs 144 s^{-1}), a reaction that is also thought to proceed via rate-limiting hydrolysis of an acyl−enzyme intermediate.[27] The alcoholytic reactions also highlight the ability of the His-Asp dyad to activate water or an alcohol. While the data do not unambiguously refute the possibility that product release is rate-determining, the observation of similar accelerations of v_0 by different alcohols suggests that this scenario is unlikely. Specifically, the limiting of turnover by product release would imply that methyl, ethyl, and propyl benzoates are released from the active site at an equal rate that is faster than that of benzoic acid. By contrast, assigning a chemical dependence to k_{cat} is consistent with the reported absence of a solvent viscosity effect during HOPDA turnover,[13] and the presence of a solvent kinetic isotope effect (sKIE) during BphD-mediated ester bond hydrolysis.[19]

The similar k_{cat} values for HOPDA and pNPB hydrolysis together with the similar partitioning of these reactions between the hydro- and alcoholytic pathways (Scheme 4) mirror what has been reported for other hydrolases that utilize a covalent mechanism. Thus, constant partition ratios have been reported in serine proteases, such as chymotrypsin,[27] and non-serine hydrolases, such as prostatic acid phosphatase,[28] all of which are proposed to proceed via acyl−enzyme intermediates. For the BphD-mediated methanol-dependent turnover of HOPDA, a simple kinetic model for a nucleophilic mechanism correctly predicted the observed increase in k_{cat} and K_m as well as the independence of k_{cat}/K_m. Furthermore, the experimentally determined product ratios from the turnover of both HOPDA and pNPB also matched the values predicted by the nucleophilic model. Collectively, the data suggest that the distinct substrates are cleaved through a shared, Ser112−benzoyl intermediate. This conclusion contradicts an earlier proposal that Ser112 acts as a hydrogen bond donor during C−O bond hydrolysis. This previously assigned role for Ser112 was deduced from a Hammet analysis using *para*-substituted pNPBs[19] and further supported using substrate docking experiments.[21] In particular, the Hammet plot was nonlinear, a feature that was attributed to a change in the rate-limiting step from ester bond cleavage to product release for substrates for which $\sigma \geq 0$. An alternative explanation for the nonlinearity is that the activation of water for nucleophilic attack on the Ser112−benzoyl ester may become rate-limiting for substrates for which $\sigma \geq 0$. This alternate explanation is consistent not only with the dependence of k_{cat} on alcohol but also with the aforementioned lack of viscosity effect and the presence of a sKIE during turnover of esters.

Transient-state kinetic analyses of catalytic triad variants of BphD indicate that the mechanism of nucleophile activation differs in pNPB and HOPDA hydrolysis, consistent with the different leaving groups of the two substrates. Thus, serinate

dx.doi.org/10.1021/bi300663r | *Biochemistry* 2012, 51, 5831−5840

formation during C−C bond cleavage was recently proposed to occur through a substrate-assisted mechanism, facilitated by an enzymatic perturbation of the electron-rich MCP dienoate.[3] Consistent with this proposal, substitution of His265 with Ala or Gln reduced the rate of acylation by only 5−40-fold during HOPDA hydrolysis, while breakdown of the acyl−enzyme intermediate remained rate-limiting.[3] In contrast, these same substitutions reduced the rate of acylation by more than 3 orders of magnitude for pNPB hydrolysis such that acylation becomes rate-limiting. This significant reduction in the rate of catalysis is similar to those observed in Ser-His-Asp triad variants of other α/β-hydrolases such as esterases[29,30] and serine proteases.[31] Both of the latter classes of hydrolases utilize covalent mechanisms of catalysis and use the His-Asp dyad for serinate formation. Our results, together with the apparent abrogation of chemistry upon substitution of Ser112 in BphD, are also consistent with a previous steady-state study of MhpC in which the S110A and H263A variants did not possess detectable esterase activity against monoethyl adipate.[18] Overall, the reduction in the rate of pNP production in the His265 variants implicates the His-Asp dyad in the activation of the serine for C−O bond hydrolysis in MCP hydrolases.

The steady-state kinetic studies of the methanol dependence of C−C bond cleavage provide additional evidence of a two-conformation model of catalysis. This model was previously proposed on the basis of biphasic product formation in BphD observed in stopped-flow analyses[13] and half-site reactivity in the wild-type enzyme.[3] According to the proposal, one form of the enzyme catalyzes C−C bond cleavage and HPD release (E), and a second, inactive form (E′ in Scheme 5) requires a

Scheme 5. Two-Conformation Model of Catalysis by the MCP Hydrolases

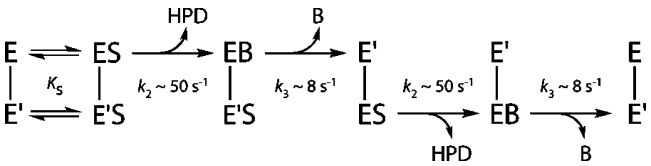

conformational change associated with a catalytic event in a linked, active subunit. Thus, the two-conformation model requires C−C bond cleavage (k_2) to occur in E (half the enzyme sites) before a conformational change converts E′ (the other half of the active sites) to E, thereby allowing catalysis to proceed in the remaining "stalled" active sites. The steady-state kinetic analysis reported herein is consistent with this two-conformation model inasmuch as the apparent rate of acylation observed at high methanol concentrations ($k_2 \sim 30\ s^{-1}$) is significantly lower than that observed via single-turnover stopped-flow experiments ($k_2 \sim 50\ s^{-1}$).[13] Whereas acylation was directly observed in the latter experiment, it is inferred from a methanol-induced change in the rate-determining step observed in the former experiments. At low methanol concentrations, k_{cat} primarily reflects rate-determining deacylation (~8 s^{-1}), the extent of which increases with methanol concentration until acylation becomes rate-determining. Therefore, in the simplified kinetic Scheme 2, when $k_{deacylation} > k_{acylation}$ (high MeOH concentration), k_{cat} should be similar to the rate of acylation. However, in the two-conformation model depicted in Scheme 5, each substrate molecule (after the first turnover) will remain enzyme-bound through two acylation−deacylation cycles. Thus, if we assume $k_{deacylation} > k_{acylation}$ at high methanol concentrations, the sum of the transit times (reciprocal rates) for two acylation steps yields a k_{cat} of ~25 s^{-1} {i.e., $1/[1/(50\ s^{-1}) + 1/(50\ s^{-1})]$}, in reasonable agreement with the fitted value of 30 s^{-1}.

The transient-state kinetic studies of pNPB hydrolysis further support the occurrence of active sites with different reactivities in BphD. Specifically, the BphD-mediated production of pNP was biphasic at 2:1 and 1:1 enzyme:substrate ratios. Amplitude analyses indicate that the relative proportion of "fast-acting" enzyme, characterized by acylation rates of 200 s^{-1}, diminished with an increasing active site occupancy and suggested that the occupancy of more than a single active site within the tetramer leads to a 5-fold reduction in the rate of pNP production from individual catalytic sites ($k_2 \sim 40\ s^{-1}$). Nevertheless, qualitative inspection of the kinetic traces did not reveal a textbook pre-steady-state burst phase even at the highest concentration of BphD tested. The poorly defined burst phase may be due, in part, to the relatively small difference in observed rates: k_{burst} ($=k_2$) ~ 40 s^{-1}, and k_{ss} ~ 8 s^{-1}. However, it may also reflect the different manner in which pNPB interacts with the active site of BphD as compared to HOPDA, which must be tautomerized prior to hydrolysis. Indeed, turnover of pNPB did not strictly conform to the two-conformation model of catalysis: the turnover was substoichiometric, and pNP production was asynchronous. Thus, during the first turnover, 60−70% of the protomers were fast-acting and the visible signal originating from the remaining 30−40% of the active sites likely contributed to a poorly defined pre-steady-state phase. Overall, these results, together with the single-turnover experiments at varying enzyme:substrate ratios, highlight a catalytic outcome of disrupting the well-conserved MCP hydrolase−substrate interactions. In similar studies monitoring the BphD-catalyzed hydrolysis of *p*-nitrophenyl acetate, no pre-steady-state kinetic burst was reported.[19] However, acetylation of Ser112 may be rate-limiting for this substrate as it shares no chemical substructure with HOPDA.

The structural basis of the half-site reactivity of MCP hydrolases remains unexplained. Although the orientation of active site residues such as Phe175, Phe239, and Trp266 can be correlated with active site occupancy,[13,32,33] it is unclear whether these different orientations alter the reactivity of the active site. Nevertheless, the crystal structures of MhpC and HsaD both revealed half-of-sites occupancy in the presence of model substrates or inhibitors,[32,33] consistent with subpopulations of active sites possessing different substrate affinities. Despite the structural variation, determination of a dissociation constant for the S114A variant of HsaD with a steroid-derived substrate suggested that the binding was stoichiometric.[33] Interestingly, the spectrum of a red-shifted catalytic intermediate, named ES^{red}, whose lifetime is extended in serine variants,[13,17,33] provides some evidence of the occurrence of two distinct active site environments in MCP hydrolases despite full occupancy. Thus, the spectrum of ES^{red} in BphD has λ_{max} values at 473 and 492 nm, suggesting contributions from two enzyme-bound species.[13] Ongoing efforts are aimed at elucidating the structural basis of half-site reactivity as well as the nature of ES^{red}.

■ ASSOCIATED CONTENT

Supporting Information

Representative HPLC chromatograms and fitting of pre-steady-state kinetic data. This material is available free of charge via the Internet at http://pubs.acs.org.

AUTHOR INFORMATION

Corresponding Author

*Address: 2350 Health Sciences Mall, Vancouver, British Columbia V6T 1Z3, Canada. Telephone: (604) 822-0042. Fax: (604) 822-6041. E-mail: leltis@mail.ubc.ca.

Present Address

†Department of Chemistry, Wilfrid Laurier University, Waterloo, Ontario, Canada.

Funding

A.C.R. is a recipient of a studentship from the National Science and Engineering Research Council (NSERC) of Canada. This work was supported by an NSERC Discovery Grant to L.D.E.

Notes

The authors declare no competing financial interest.

ACKNOWLEDGMENTS

We thank Dr. Jeffrey T. Bolin for helpful discussion.

ABBREVIATIONS

DxnB2, 2,8-dihydroxy-6-oxo-6-phenylhexa-2,4-dienoate 5,6-hydrolase; BphD, 2-hydroxy-6-oxo-6-phenylhexa-2,4-dienoate 5,6-hydrolase; MhpC, 2-hydroxy-6-oxonona-2,4-diene-1,9-dioic acid 5,6-hydrolase; HOPDA, 2-hydroxy-6-oxo-6-phenylhexa-2,4-dienoate; pNPB, *p*-nitrophenyl benzoate; pNP, *p*-nitrophenol; v_0, initial velocity; sKIE, solvent kinetic isotope effect.

REFERENCES

(1) Seah, S. Y., Labbe, G., Nerdinger, S., Johnson, M. R., Snieckus, V., and Eltis, L. D. (2000) Identification of a serine hydrolase as a key determinant in the microbial degradation of polychlorinated biphenyls. *J. Biol. Chem. 275*, 15701−15708.

(2) Rengarajan, J., Bloom, B. R., and Rubin, E. J. (2005) Genome-wide requirements for *Mycobacterium tuberculosis* adaptation and survival in macrophages. *Proc. Natl. Acad. Sci. U.S.A. 102*, 8327−8332.

(3) Ruzzini, A. C., Ghosh, S., Horsman, G. P., Foster, L. J., Bolin, J. T., and Eltis, L. D. (2012) Identification of an Acyl-Enzyme Intermediate in a *meta*-Cleavage Product Hydrolase Reveals the Versatility of the Catalytic Triad. *J. Am. Chem. Soc. 134*, 4615−4624.

(4) Ollis, D. L., Cheah, E., Cygler, M., Dijkstra, B., Frolow, F., Franken, S. M., Harel, M., Remington, S. J., Silman, I., Schrag, J., et al. (1992) The α/β-hydrolase fold. *Protein Eng. 5*, 197−211.

(5) Nardini, M., and Dijkstra, B. W. (1999) α/β-Hydrolase fold enzymes: The family keeps growing. *Curr. Opin. Struct. Biol. 9*, 732−737.

(6) Jiang, Y., Morley, K. L., Schrag, J. D., and Kazlauskas, R. J. (2011) Different active-site loop orientation in serine hydrolases versus acyltransferases. *ChemBioChem 12*, 768−776.

(7) Holmquist, M. (2000) α/β-Hydrolase fold enzymes: Structures, functions and mechanisms. *Curr. Protein Pept. Sci. 1*, 209−235.

(8) Gruber, K., Gartler, G., Krammer, B., Schwab, H., and Kratky, C. (2004) Reaction mechanism of hydroxynitrile lyases of the α/β-hydrolase superfamily: The three-dimensional structure of the transient enzyme-substrate complex certifies the crucial role of Lys236. *J. Biol. Chem. 279*, 20501−20510.

(9) Frerichs-Deeken, U., Ranguelova, K., Kappl, R., Huttermann, J., and Fetzner, S. (2004) Dioxygenases without requirement for cofactors and their chemical model reaction: Compulsory order ternary complex mechanism of 1H-3-hydroxy-4-oxoquinaldine 2,4-dioxygenase involving general base catalysis by histidine 251 and single-electron oxidation of the substrate dianion. *Biochemistry 43*, 14485−14499.

(10) Larsen, N. A., Lin, H., Wei, R., Fischbach, M. A., and Walsh, C. T. (2006) Structural characterization of enterobactin hydrolase IroE. *Biochemistry 45*, 10184−10190.

(11) Fleming, S. M., Robertson, T. A., Langley, G. J., and Bugg, T. D. (2000) Catalytic mechanism of a C-C hydrolase enzyme: Evidence for a gem-diol intermediate, not an acyl enzyme. *Biochemistry 39*, 1522−1531.

(12) Li, J. J., Li, C., Blindauer, C. A., and Bugg, T. D. (2006) Evidence for a gem-diol reaction intermediate in bacterial C-C hydrolase enzymes BphD and MhpC from ^{13}C NMR spectroscopy. *Biochemistry 45*, 12461−12469.

(13) Horsman, G. P., Ke, J., Dai, S., Seah, S. Y., Bolin, J. T., and Eltis, L. D. (2006) Kinetic and structural insight into the mechanism of BphD, a C-C bond hydrolase from the biphenyl degradation pathway. *Biochemistry 45*, 11071−11086.

(14) Li, C., Li, J. J., Montgomery, M. G., Wood, S. P., and Bugg, T. D. (2006) Catalytic role for arginine 188 in the C-C hydrolase catalytic mechanism for *Escherichia coli* MhpC and *Burkholderia xenovorans* LB400 BphD. *Biochemistry 45*, 12470−12479.

(15) Lam, W. W., and Bugg, T. D. (1997) Purification, characterization, and stereochemical analysis of a C-C hydrolase: 2-Hydroxy-6-keto-nona-2,4-diene-1,9-dioic acid 5,6-hydrolase. *Biochemistry 36*, 12242−12251.

(16) Henderson, I. M., and Bugg, T. D. (1997) Pre-steady-state kinetic analysis of 2-hydroxy-6-keto-nona-2,4-diene-1,9-dioic acid 5,6-hydrolase: Kinetic evidence for enol/keto tautomerization. *Biochemistry 36*, 12252−12258.

(17) Horsman, G. P., Bhowmik, S., Seah, S. Y., Kumar, P., Bolin, J. T., and Eltis, L. D. (2007) The tautomeric half-reaction of BphD, a C-C bond hydrolase. Kinetic and structural evidence supporting a key role for histidine 265 of the catalytic triad. *J. Biol. Chem. 282*, 19894−19904.

(18) Li, C., Montgomery, M. G., Mohammed, F., Li, J. J., Wood, S. P., and Bugg, T. D. (2005) Catalytic mechanism of C-C hydrolase MhpC from *Escherichia coli*: Kinetic analysis of His263 and Ser110 site-directed mutants. *J. Mol. Biol. 346*, 241−251.

(19) Li, J. J., and Bugg, T. D. (2007) Investigation of a general base mechanism for ester hydrolysis in C-C hydrolase enzymes of the α/β-hydrolase superfamily: A novel mechanism for the serine catalytic triad. *Org. Biomol. Chem. 5*, 507−513.

(20) Li, C., Hassler, M., and Bugg, T. D. (2008) Catalytic promiscuity in the α/β-hydrolase superfamily: Hydroxamic acid formation, C−C bond formation, ester and thioester hydrolysis in the C−C hydrolase family. *ChemBioChem 9*, 71−76.

(21) Zhou, H., Qu, Y., Kong, C., Wu, Y., Zhu, K., Yang, J., and Zhou, J. (2012) Promiscuous esterase activities of the C-C hydrolases from *Dyella ginsengisoli*. *Biotechnol. Lett. 34*, 1107−1113.

(22) Seah, S. Y., Terracina, G., Bolin, J. T., Riebel, P., Snieckus, V., and Eltis, L. D. (1998) Purification and preliminary characterization of a serine hydrolase involved in the microbial degradation of polychlorinated biphenyls. *J. Biol. Chem. 273*, 22943−22949.

(23) Cornish-Bowden, A. (1995) *Analysis of enzyme kinetic data*, Oxford University Press, New York.

(24) Li, J., Szittner, R., Derewenda, Z. S., and Meighen, E. A. (1996) Conversion of serine-114 to cysteine-114 and the role of the active site nucleophile in acyl transfer by myristoyl-ACP thioesterase from *Vibrio harveyi*. *Biochemistry 35*, 9967−9973.

(25) Nazi, I., and Wright, G. D. (2005) Catalytic mechanism of fungal homoserine transacetylase. *Biochemistry 44*, 13560−13566.

(26) Bhowmik, S., Horsman, G. P., Bolin, J. T., and Eltis, L. D. (2007) The molecular basis for inhibition of BphD, a C-C bond hydrolase involved in polychlorinated biphenyls degradation: Large 3-substituents prevent tautomerization. *J. Biol. Chem. 282*, 36377−36385.

(27) Fastrez, J., and Fersht, A. R. (1973) Demonstration of the acyl-enzyme mechanism for the hydrolysis of peptides and anilides by chymotrypsin. *Biochemistry 12*, 2025−2034.

(28) Ostrowski, W., and Barnard, E. A. (1973) Evidence for a phosphoryl-enzyme intermediate in the catalytic reaction of prostatic acid phosphatase. *Biochemistry 12*, 3893−3898.

(29) Padhi, S. K., Fujii, R., Legatt, G. A., Fossum, S. L., Berchtold, R., and Kazlauskas, R. J. (2010) Switching from an esterase to a

hydroxynitrile lyase mechanism requires only two amino acid substitutions. *Chem. Biol. 17*, 863−871.
(30) Lai, K. K., Stogios, P. J., Vu, C., Xu, X., Cui, H., Molloy, S., Savchenko, A., Yakunin, A., and Gonzalez, C. F. (2011) An inserted α/β subdomain shapes the catalytic pocket of *Lactobacillus johnsonii* cinnamoyl esterase. *PLoS One 6*, e23269.
(31) Corey, D. R., and Craik, C. S. (1992) An investigation into the minimum requirements for peptide hydrolysis by mutation of the catalytic triad of trypsin. *J. Am. Chem. Soc. 114*, 1784−1790.
(32) Dunn, G., Montgomery, M. G., Mohammed, F., Coker, A., Cooper, J. B., Robertson, T., Garcia, J. L., Bugg, T. D., and Wood, S. P. (2005) The structure of the C-C bond hydrolase MhpC provides insights into its catalytic mechanism. *J. Mol. Biol. 346*, 253−265.
(33) Lack, N. A., Yam, K. C., Lowe, E. D., Horsman, G. P., Owen, R. L., Sim, E., and Eltis, L. D. (2010) Characterization of a carbon-carbon hydrolase from *Mycobacterium tuberculosis* involved in cholesterol metabolism. *J. Biol. Chem. 285*, 434−443.